JOURNAL OF CATALYSIS 82, 127–146 (1983)

The Sintering of an Alumina-Supported Platinum Catalyst Studied by Transmission Electron Microscopy

P. J. F. HARRIS,* E. D. BOYES,* AND J. A. CAIRNS†

*Department of Metallurgy and Science of Materials, University of Oxford, Parks Road, Oxford OX1 3PH, England, and †Chemistry Division, AERE Harwell, Didcot, Oxfordshire OX11 ORA, England

Received July 29, 1982; accepted February 15, 1983

Specimens of a commercial platinum/alumina catalyst were prepared for transmission electron microscopy by a new technique based on the sol-gel process. Sintering of supported particles in specimens heated at 600°C in air was investigated. An examination of sintering data suggested that a change in the predominant sintering mechanism occurred after approximately 2 hr. In specimens heated for 8 hr or longer, anomalously large (>200 Å) particles were commonly observed. Analyses of such particles by X-ray microanalysis and convergent beam electron diffraction were consistent with metallic platinum. Average particle diameters determined by microscopy were corroborated by surface area measurement using the H_2 pulse-flow method.

INTRODUCTION

Metal particle sintering plays a major rôle in the deactivation of supported metal catalysts. This has been established in a large number of studies using a variety of techniques, chiefly X-ray diffraction, selective chemisorption, and transmission electron microscopy (TEM). A study of noble metal automotive oxidation catalysts using CO adsorption and TEM (*1*), for example, has shown that sintering can result in a 95% loss of available metal surface area. However, while the evidence for sintering is well documented, the mechanism is imperfectly understood and has been the subject of much discussion in the literature. Several attempts have been made to develop mechanistic models to account for sintering behavior. These models may be grouped into two types: those which envisage growth through the random migration of metal particles across the support surface followed by collision and coalescence (*2–4*), and those which involve migration of single metal atoms (or molecular species) from small particles to large ones (*5–9*). The aim of these models is to predict kinetic parameters for the sintering process and to discuss in general terms how the metal particle size distribution should change with time.

There have been numerous attempts to elucidate the mechanism through TEM studies of "model" catalysts, usually comprising metal particles evaporated onto a carbon or oxide film (e.g., *7, 10–16*). While some of these studies have led to indications of the predominant sintering mechanism, the relationship of sintering behavior in idealized systems to that in commercial catalysts with a different form of substrate (support) has not been well established. Clearly, a program of TEM studies of sintering in "real" catalysts could be of great value. It is surprising, therefore, that relatively few such studies of commercial oxide-supported catalysts have appeared in the literature (*1, 17–22*). This is probably due to the difficulties involved in preparing TEM specimens from these hard, porous materials. Traditional specimen preparation techniques have entailed either depositing some of the powdered catalyst onto a carbon film (*23, 24*) or alternatively setting the catalyst in a resin and sectioning with an ultramicrotome (*25*). Both procedures may result in some disruption of the origi-

0021-9517/83 $3.00

nal catalyst morphology, and sufficiently thin regions are often difficult to obtain.

In this study a new specimen preparation technique, which avoids these difficulties, is applied to a commercial platinum/alumina catalyst. The technique involves mixing an aqueous solution of a platinum complex with an alumina sol, i.e., an aqueous dispersion of colloidal particulates (*26*), and dip-coating a microscope grid with this material. After drying, firing, and reducing, thin films of catalyst suitable for microscopy are formed across the grid. A similar technique has recently been applied to a study of ceria gels (*27*).

Specimens prepared by the new technique were subjected to a series of heat treatments in air at 600°C. This combination of atmosphere and temperature was chosen to represent a first approximation to conditions experienced by catalysts in an automobile exhaust train (*28*). Results of the sintering experiments are discussed with reference to existing theoretical models. Characterization of some of the larger particles is carried out by X-ray microanalysis and convergent beam electron diffraction. Finally, values of the surface average diameter determined by TEM are compared with surface area measurements carried out by the H_2 pulse-flow method.

EXPERIMENTAL

Transmission electron microscopy. Specimens containing Pt/Al_2O_3 in the proportion 1 : 15 by weight were prepared as follows. Tetrammine platinous chloride (0.769 g) (Johnson Matthey and Co. Ltd.) was dissolved in the minimum of water and mixed with 25 ml of an aqueous colloidal sol containing 270 g η-alumina per liter, to which a wetting agent had been added to facilitate formation of a catalyst film. Further mixing was carried out in an ultrasonic bath. Stainless-steel TEM grids (100 mesh) were then dipped into the mixture and withdrawn with a film of the catalyst precursor suspended across the squares of the grid. This was then dried at 80°C, fired at 600°C in air for 30 min, and reduced in a stream of flowing hydrogen at 500°C for 1 hr. In this way extremely thin sheet-like regions were formed across parts of the grid squares. Freshly reduced specimens were subjected to heat treatments of 0.5, 2, 8, 16, and 24 hr in air at 600°C.

The microscope, a Philips EM 300G instrument, was operated in bright field mode at a calibrated magnification of 213,000× (±3%) for the study of particle sintering; this enabled particles as small as 10 Å to be imaged. Flynn *et al.* (*29*) and Treacy and Howie (*30*) have pointed out that care must be exercised in the interpretation of images from particles smaller than about 20 Å in diameter due to, among other things, phase-contrast effects. However, this did not constitute a serious drawback in the present study since most of the particles were larger than this critical size. Platinum particle diameters were measured on prints enlarged ×3 from the plates, making an overall magnification of 640,000×. Particle size distributions were developed by dividing the size range into 10-Å increments (this being the lowest meaningful division of diameters suggested by Flynn *et al.* (*29*)) and assigning each particle to one of these ranges. A population of 1000 particles was measured in this way on micrographs of several different areas from at least six specimens which had undergone a given heat treatment; 2000 particles were measured in fresh specimens. For each heat treatment the number average diameter, d_n, and the surface average diameter, d_s, were determined. These parameters are defined as follows (*23*):

$$d_n = \frac{\Sigma n_i d_i}{\Sigma n_i} \qquad d_s = \frac{\Sigma n_i d_i^3}{\Sigma n_i d_i^2}$$

where n_i = number of particles in diameter increment with mid-point of d_i Å.

The surface average diameter is the weighted value such that if all the particles were spherical and of this size, then this would produce the observed surface area.

It is therefore the most useful parameter to relate to surface area measurements.

Convergent beam electron diffraction and X-ray microanalysis. Convergent beam electron diffraction patterns of individual platinum particles were obtained using a Philips EM 400T microscope in "microdiffraction" mode. A focused spot was obtained by increasing the excitation of the first condenser lens while making suitable adjustments to the second condenser lens in the way described by Steeds (*31*). Convergent beam experiments were confined to the larger particles in heavily sintered specimens. Some of these large particles were also analyzed using an energy dispersive X-ray analyzer (EDX).

Surface area measurement. Platinum surface area was determined by the pulse-flow hydrogen adsorption technique described by Freel (*24*). The apparatus comprised a modified Perkin-Elmer Sigma 1 gas chromatograph with a facility for automatic injection of hydrogen slugs into an argon carrier gas stream (*32*). Catalyst samples were prepared by coating sections of Fecralloy[1] steel (*26, 33, 34*) with platinum/alumina sol and then drying, firing, and reducing these under the same conditions as for TEM specimens. Measurements were carried out on fresh samples and on samples which had been aged in air at 600°C for 2, 8, and 24 hr. Pretreatment consisted of flushing the sample tube with hydrogen at 500°C for 1 hr, followed by argon at 500°C for 1 hr; TEM measurements indicated that this would cause negligible sintering. The sample was allowed to cool to 25°C under flowing argon, and 0.1-ml slugs of H_2 were then injected. Several repeat runs were carried out on different samples which had undergone a given heat treatment.

Surface areas were calculated assuming a spherical approximation to the particle geometry, an adsorption stoichiometry of unity, and a Pt surface atom density of 1.12×10^{15} atoms/cm^2 (*24*). This led to a determination of d_s, the surface average diameter, which could be directly compared with the value from TEM.

The surface area of the alumina was 100 m^2/g, as determined by a standard BET measurement.

RESULTS AND DISCUSSION

Specimen Characteristics

Approximately 50% of specimens prepared by the new technique contained regions sufficiently thin to be useful for microscopy. Figure 1 illustrates a typical sheet-like region in a fresh specimen, while Fig. 2 shows the same region at higher magnification. Such regions were sometimes found to be unstable under a focused electron beam, but in most cases instability did not constitute a major problem.

Treacy and Howie (*30*) and Flynn *et al.* (*29*) have described the variations in particle contrast with specimen orientation that can occur as a result of amplitude contrast effects. These variations were commonly observed in the present study, but tilting experiments suggested that they would rarely cause a particle to become indistinguishable from the support. Contrast effects often resulted in smaller particles (<100 Å) appearing "transparent"; this is not taken to imply necessarily a raft-like morphology. A significant proportion of particles exhibited internal structural features such as twin boundaries. Figure 3a illustrates a singly twinned particle while Figs. 3b and c show examples of the less commonly observed multiply twinned particles. Such particles, which have been observed in previous studies of commercial catalysts (*35, 36*), would be more clearly imaged under dark-field conditions. However, for the catalyst studied here overlapping of the diffraction rings from platinum and alumina makes dark-field imaging of particles difficult.

External particle shape varied considerably. As a general rule, particles smaller

[1] Fecralloy steel is a registered trade mark of the United Kingdom Atomic Energy Authority for a specific range of steels.

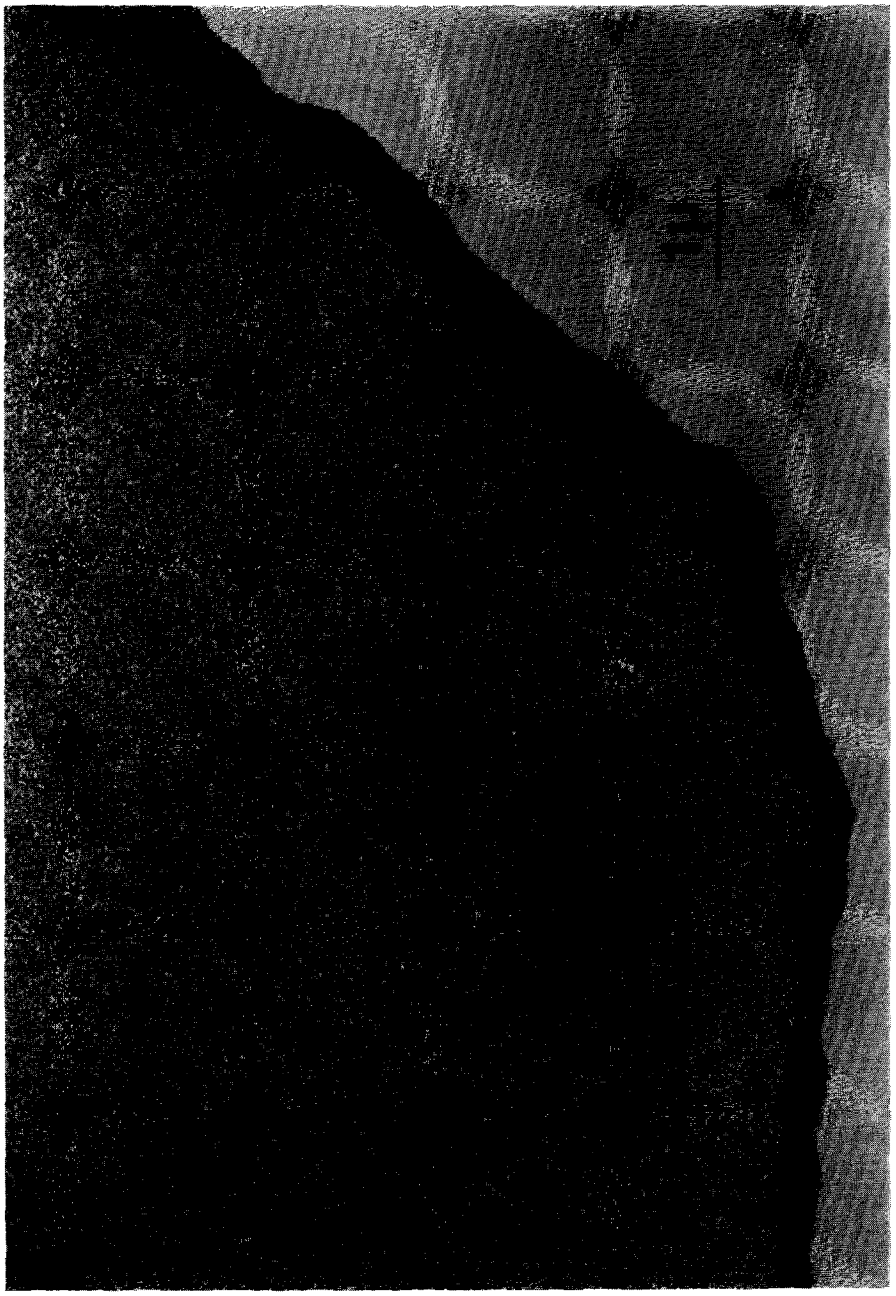

FIG. 1. Freshly reduced Pt/Al_2O_3 catalyst specimen: low magnification micrograph of typical thin region.

FIG. 2. Typical thin region of freshly reduced Pt/Al_2O_3 specimen.

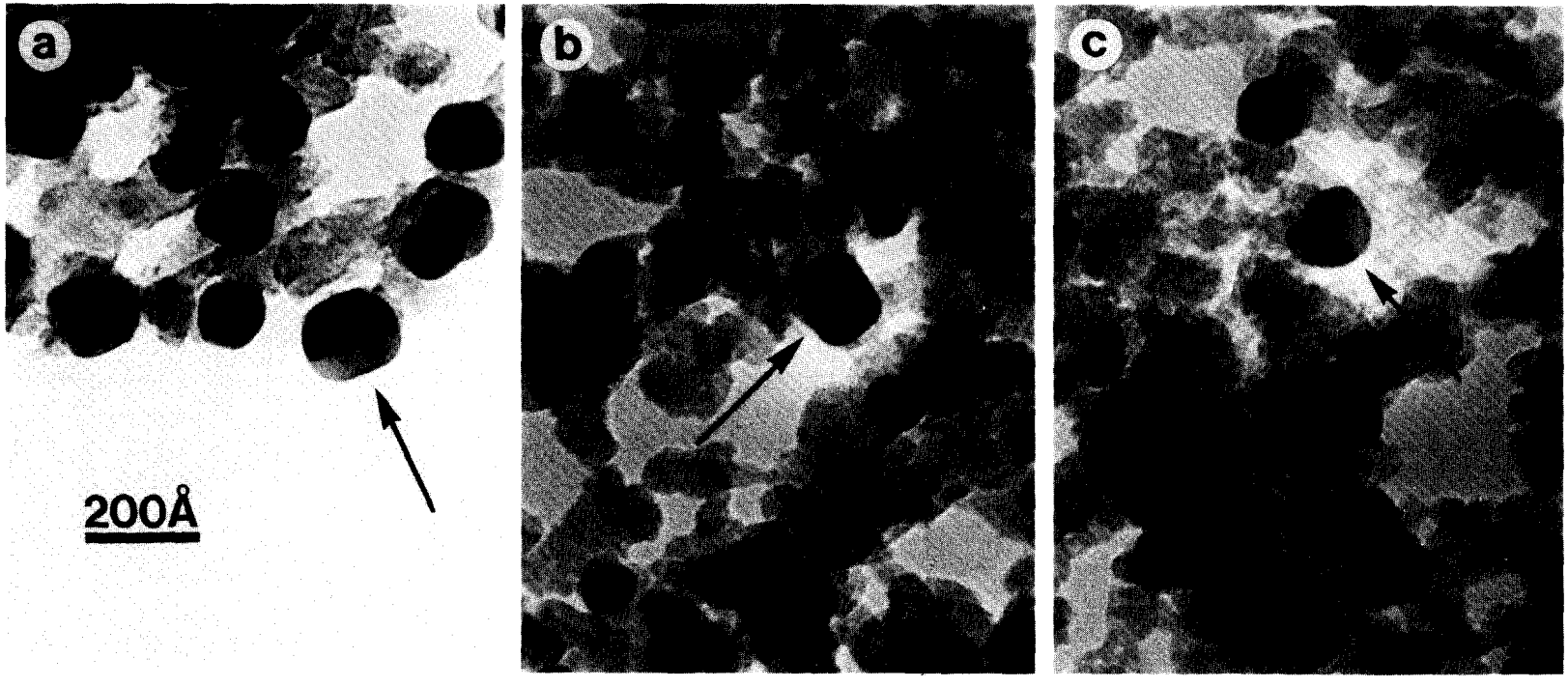

FIG. 3. Twinned platinum particles in sintered catalysts. (a) singly twinned particle; (b) and (c) multiply twinned particles.

than 50 Å appeared approximately circular in projection, while some degree of facetting became increasingly prevalent for particles larger than this size. Some of the fast-growing particles discussed in the next section exhibited a plate-like morphology; this was established by tilting experiments.

Metal Particle Sintering

Figures 4a–d illustrate the growth of platinum particles in specimens heated at 600°C in air for periods up to 24 hr. The particle size distributions (PSD) corresponding to fresh specimens and to heat treatments of 0.5, 2, 8, 16, and 24 hr are presented in Figs. 5a–f; Table 1 gives the values of d_n, the number average diameter, for these heat treatments. In this section, the shapes of the size distributions will be discussed in terms of the theoretical predictions and some conclusions will be drawn about the mechanism of sintering. The kinetic order of the sintering process will also be discussed.

The statistical model of Granqvist and Buhrman (*4*) predicts that growth by particle migration and coalescence should lead to "log-normal" size distributions. The PSDs presented here have been fitted to log-normal distribution functions (LNDF) in the way suggested (*4*), and good fits were obtained for the freshly reduced catalysts and catalysts heated for 0.5 and 2 hr (Figs. 5a–c). The fit becomes progressively less satisfactory, however, for longer sintering times (Figs. 5d–f). In terms of the Granqvist and Buhrman theory, this would suggest that particle migration and coalescence plays a predominant rôle for heat treatments less than 2 hr in duration, while an alternative mechanism becomes more important after this time. Further evidence that migration and coalescence is at least partly responsible for sintering is provided by considering the behavior of particles smaller than 40 Å in diameter. Freshly reduced specimens contain a high proportion of particles which fall into the 10–20, 20–30, and 30–40 Å ranges. The relative proportion of such particles decreases when specimens are heated for 0.5 and 2 hr, and after 8 hr no particles smaller than 40 Å are detected. This would appear to be inconsistent with the interparticle transport models (*5–9*), which postulate that particles smaller than a variable "critical size" should shrink, resulting in a permanent non-zero concentration of the smallest particles. The likely explanation, therefore, for the disappearance of particles <40 Å is that migration and coalescence occurs very rapidly for such particles. Wynblatt and Gjostein (*5*) using formulas derived by Gruber (*37*) for the migration of pores in solids, have concluded that nonfacetted particles smaller than about 100 Å should indeed migrate considerable distances at 600°C: a 50 Å particle, for example, would be expected to move 3300 Å in 5 hr. This distance is well in excess of the typical particle separation in fresh specimens (roughly 150 Å), and would suggest that collision and coalescence is the probable mechanism for the growth of the smaller particles, even when the heterogeneous nature of the support is taken into account.

If we now consider the PSD corresponding to a heat treatment of 8 hr (Fig. 5d), we find that the peak has become approximately Gaussian in shape, centered on ~85 Å, with a long tail extending to 390 Å. After 16 and 24 hr (Figs. 5e and f), the peak moves very little, becoming centered on 95 Å, and further sintering occurs mainly through the growth of large particles (>200

TABLE 1

Mean Platinum Particle Sizes for Catalysts Heated in Air at 600°C, with 95% Confidence Limits

Sintering time (hr)	Number average diameter d_n (Å)
0	49.8 ± 1.0
0.5	66.0 ± 1.6
2	73.5 ± 1.6
8	95.3 ± 2.0
16	103 ± 3
24	109 ± 3

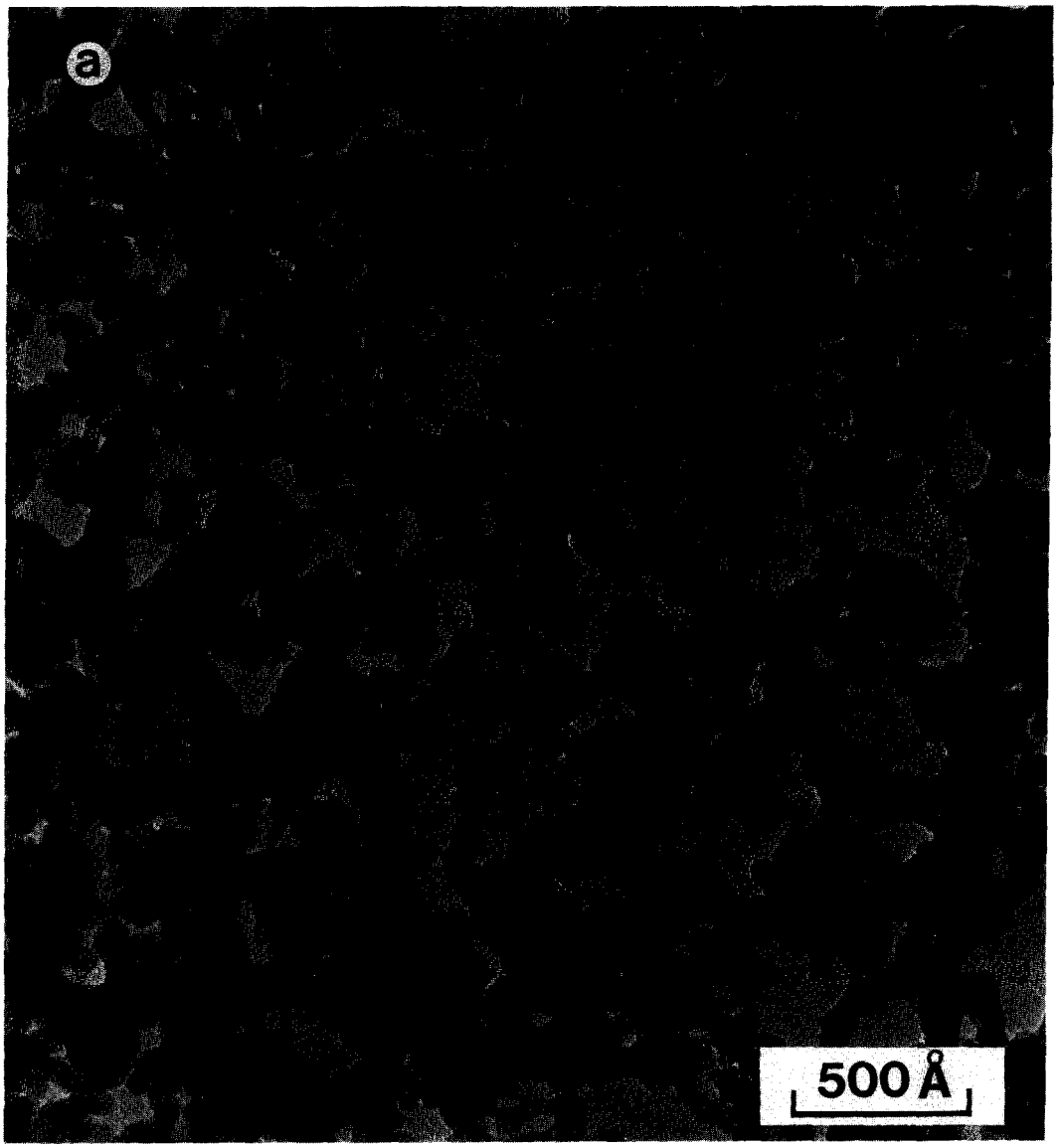

FIG. 4. Typical micrographs illustrating particle growth in Pt/Al_2O_3. (a) Freshly reduced; (b) heated in air at 600°C for 2 hr; (c) heated for 8 hr; (d) heated for 24 hr.

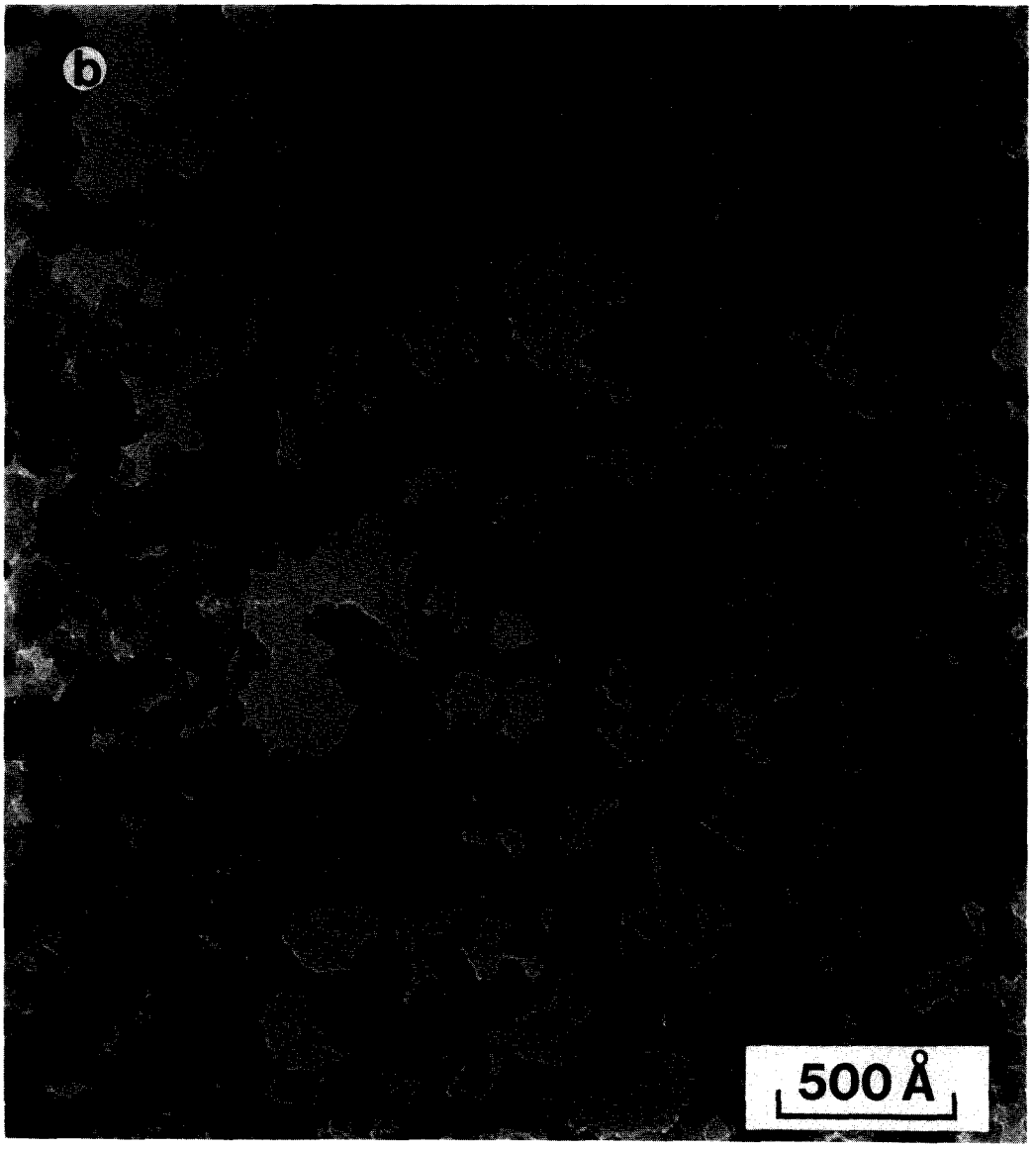

FIG. 4—*Continued.*

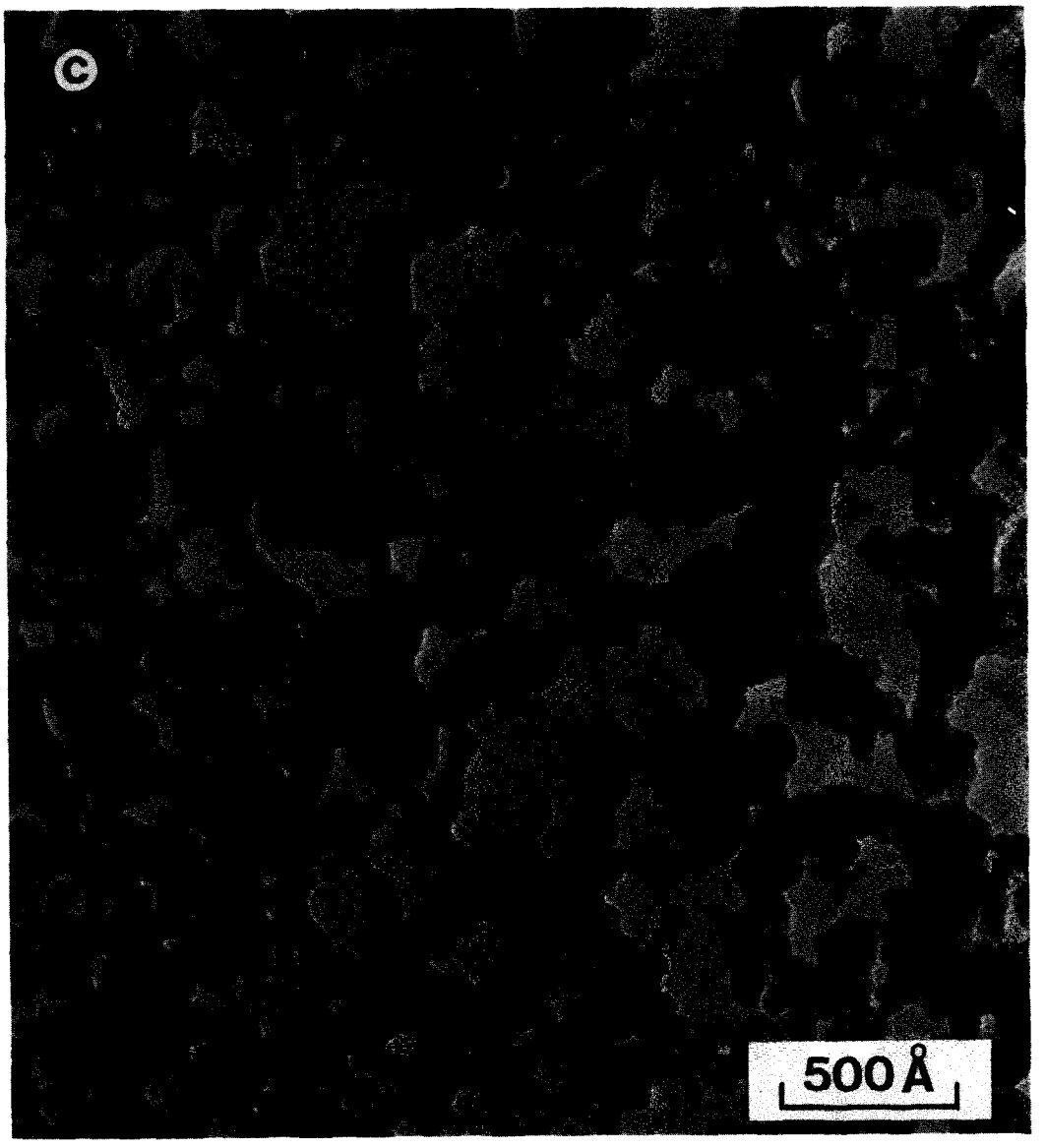

FIG. 4—*Continued.*

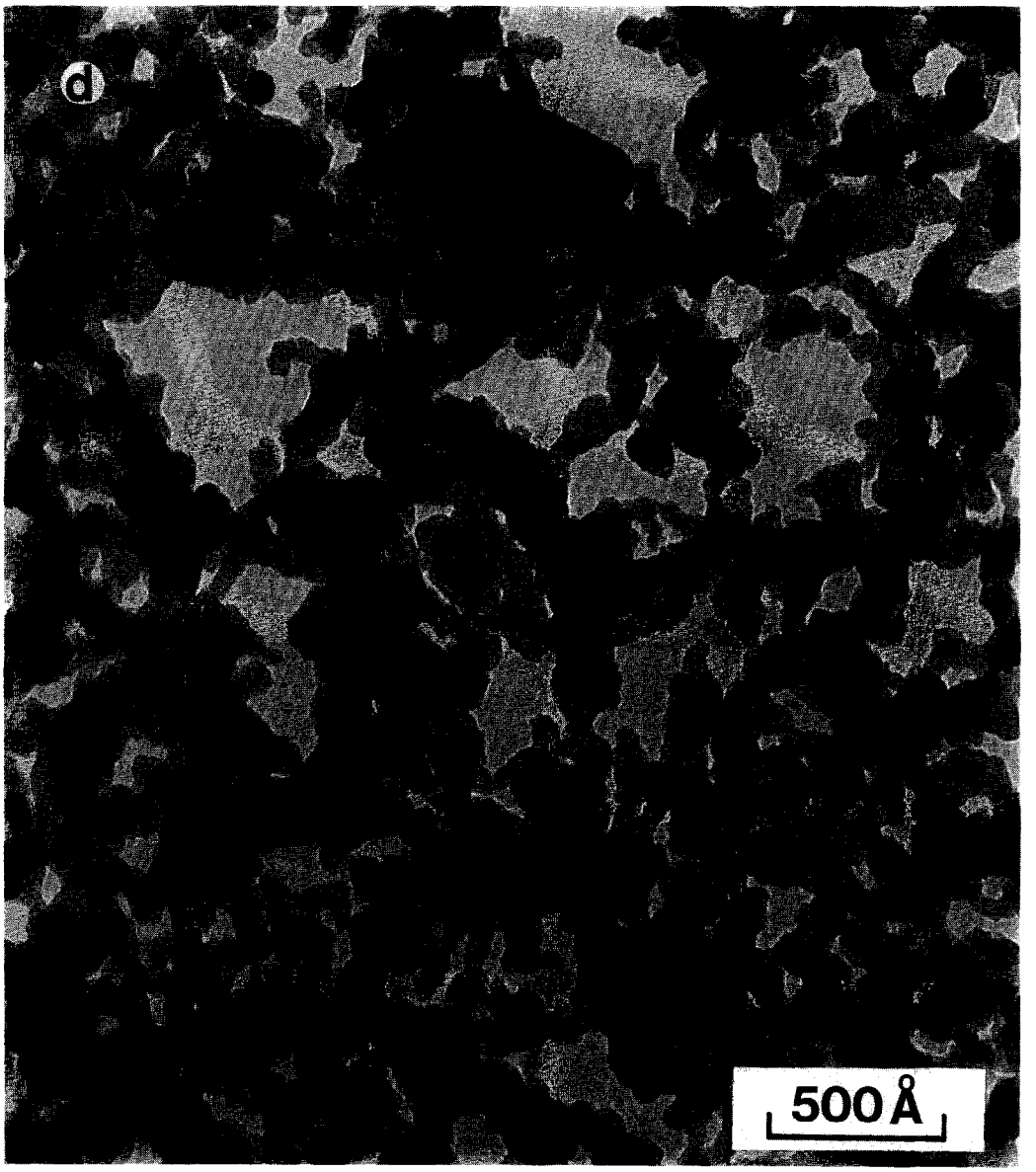

FIG. 4—*Continued.*

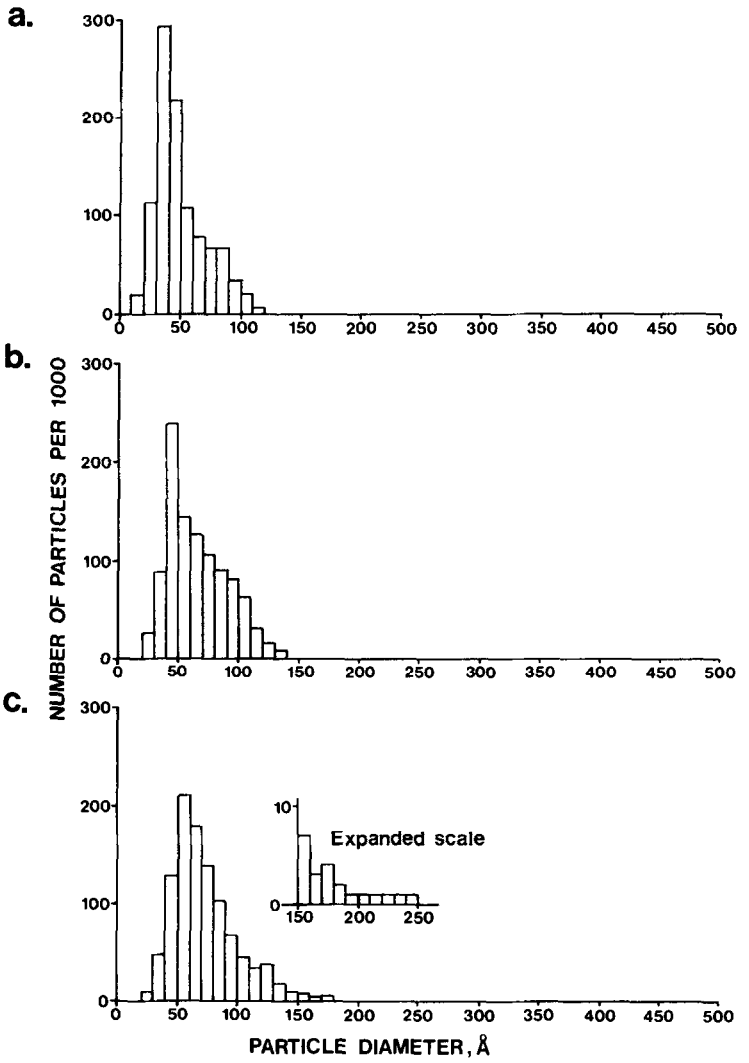

FIG. 5. Platinum particle size distributions in Pt/Al_2O_3. (a) Freshly reduced; (b) heated in air at 600°C for 30 min; (c) heated for 2 hr; (d) heated for 8 hr; (e) heated for 16 hr; (f) heated for 24 hr.

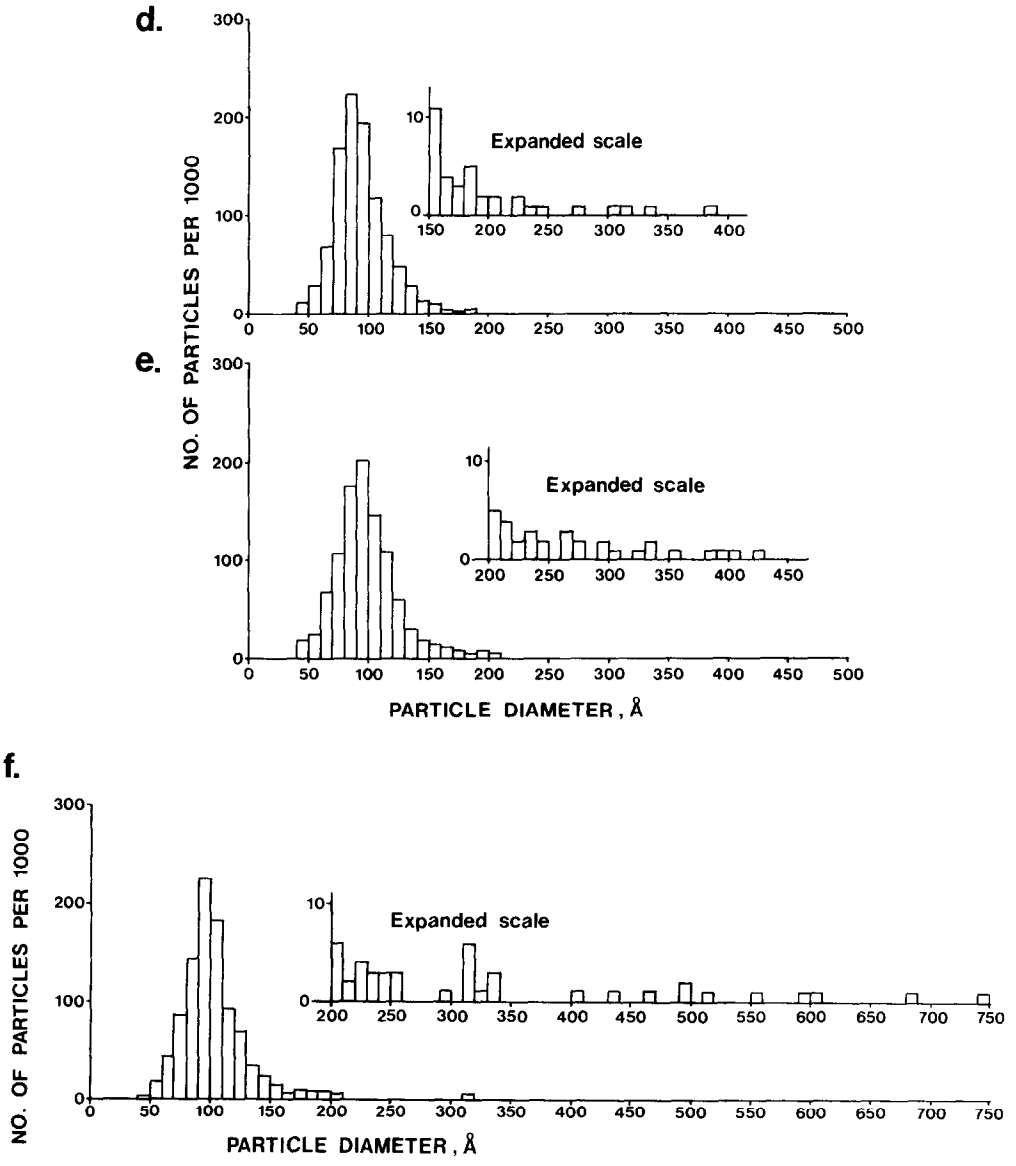

FIG. 5—*Continued.*

Å), resulting in a progressively longer tail toward the high diameter side. Figure 6 shows a number of such large particles, which were frequently facetted and sometimes exhibited a plate-like morphology. Wynblatt has observed similar "abnormally large" particles in sintered Pt/Al_2O_3 model catalysts (*7*) and Roth has recently studied the phenomenon in a commercial Pt/Al_2O_3 catalyst (*22*). PSDs with long tails to the high diameter side have also been reported in an X-ray diffraction study of commercial Ni/SiO_2 catalysts by Kuo *et al.* (*38*). The phenomenon is difficult to explain fully by a particle migration and coalescence model; the most plausible explanation is that sug-

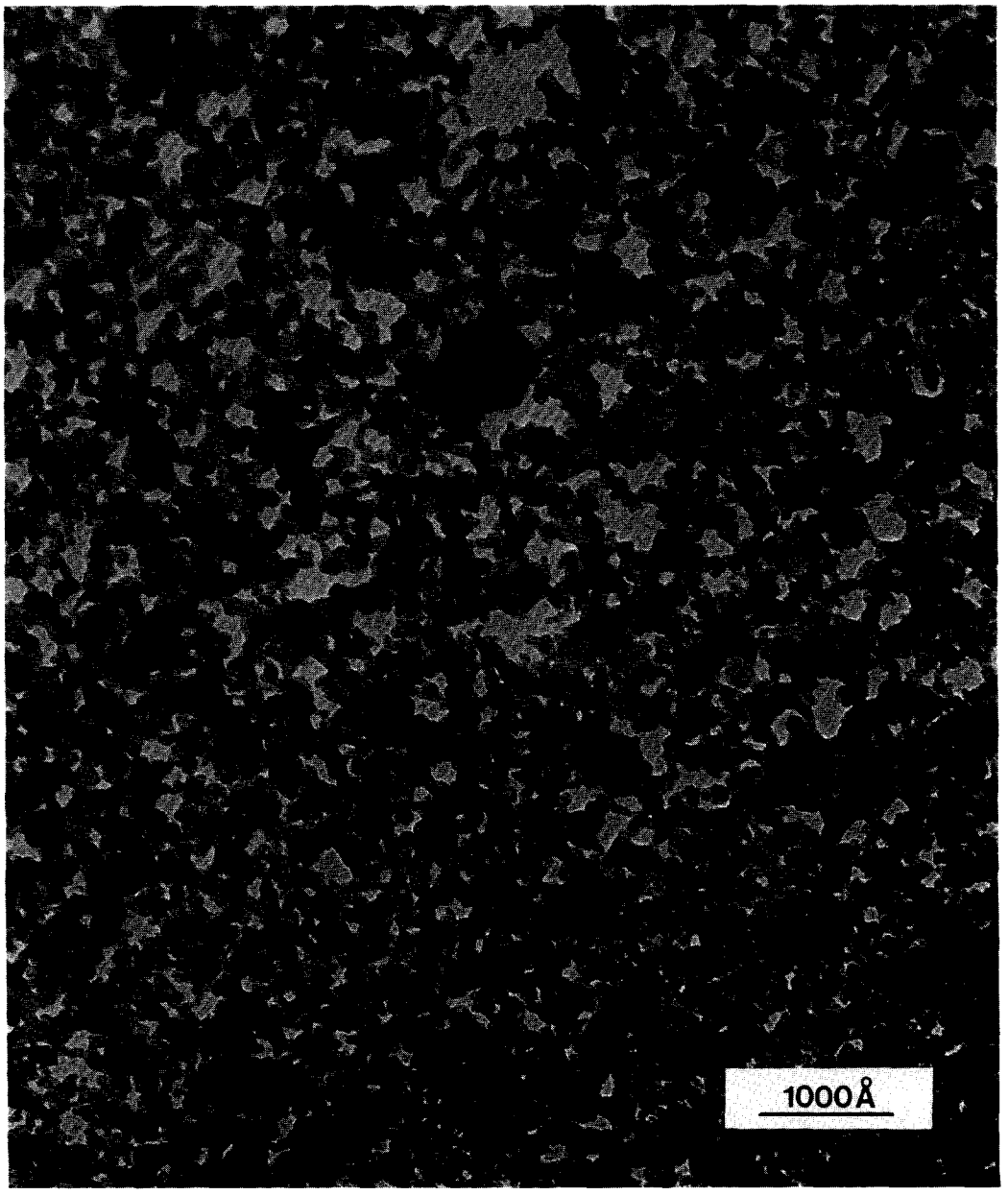

FIG. 6. Abnormally large particles in Pt/Al_2O_3 heated in air at 600°C for 24 hr.

gested by Wynblatt (*7*), namely, that fast-growing particles contain some crystallographic characteristic which facilitates growth by an interparticle transport mechanism.

Thus an analysis of the PSDs leads to the likely conclusion that for periods up to 2 hr sintering occurs chiefly by a particle migration and coalescence mechanism and that interparticle transport becomes increasingly predominant for longer periods. Further confirmation that a mechanism change occurs is provided by a consideration of the kinetic order of the process. Wynblatt and Gjostein (*5*) have stated that particle growth kinetics can be represented by an expression of the type:

$$n \log \left(\frac{R}{R_0}\right) = \log t + c$$

where R_0 is the mean particle radius in fresh specimens, R is the mean radius at time t, and c is a constant. Thus a plot of log (R/R_0) vs log t yields a value for n, and the sintering order is then $(n + 1)$. Figure 7 shows such a plot for the results set out in Table 1 and clearly demonstrates that the order changes from ~14 to ~7 after 2 hr. Several of the published theoretical models of particle migration and coalescence (*2, 3*) and of interparticle transport (*5, 6, 8, 9*) have attempted to predict the order of sintering, with results which are contradictory and inconclusive. However, in interpreting the present data it seems reasonable to conclude that a change from high to low order indicates a change from the particle migration and coalescence mechanism to the interparticle transport mechanism. Kuo *et al.* drew a similar conclusion from their X-ray diffraction data (*38*).

Analysis of Fast-Growing Particles

Previous studies have reported microdiffraction patterns of small (<100 Å) (*39, 40*) and large (>250 Å) (*22*) metal particles in commercial catalysts. In the present study convergent beam diffraction patterns were obtained from "abnormally large" particles in specimens heated for 24 hr in air at 600°C. It was found that particles which protruded from the edge of a crack in the specimen provided the best patterns. However, specimen instability under a highly focused electron beam proved to be a serious problem when attempting to record such

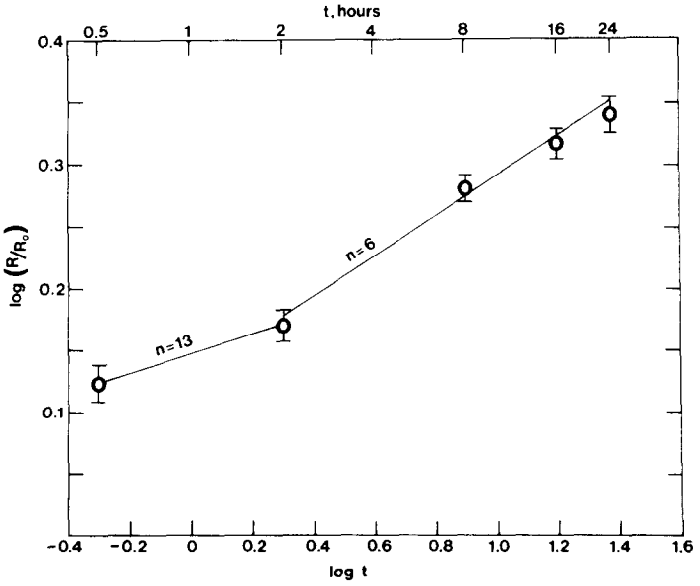

FIG. 7. Plot of log (R/R_0) vs log t for Pt/Al_2O_3 sintered in air at 600°C.

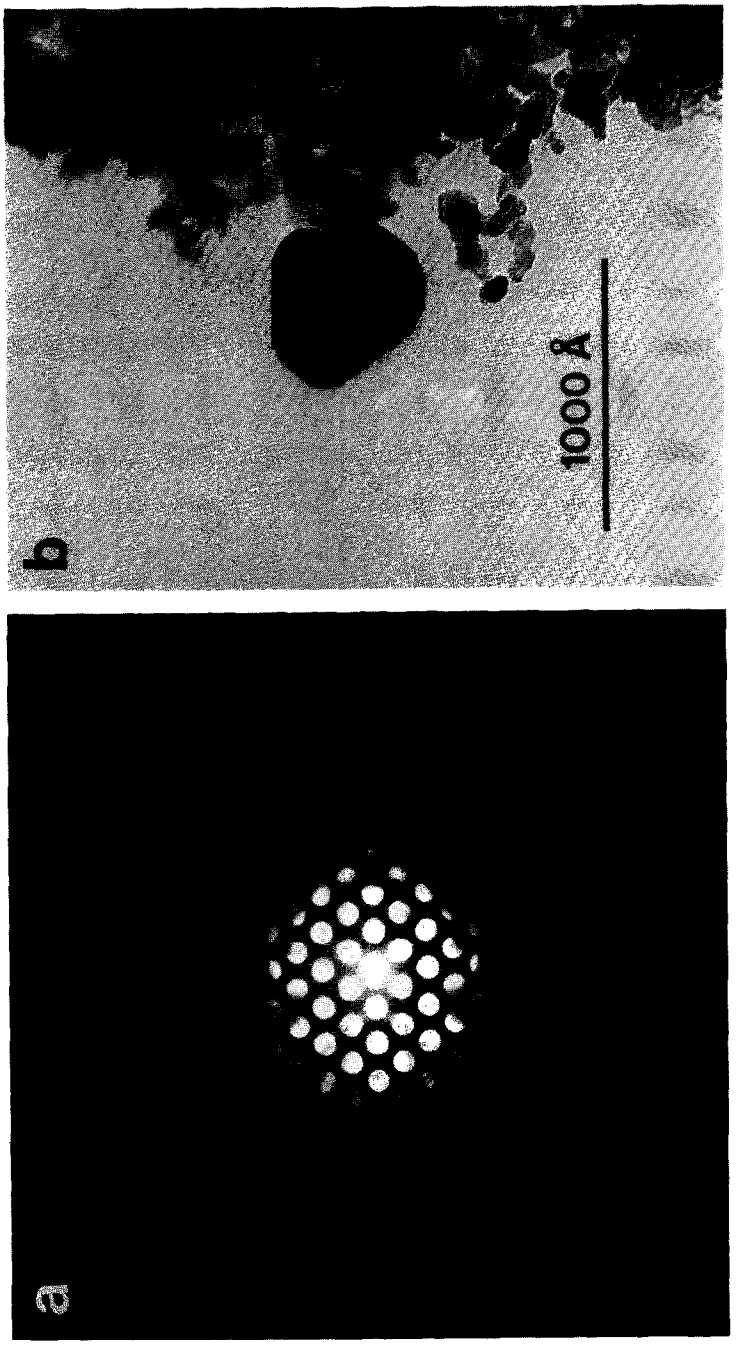
1000 Å
a
b

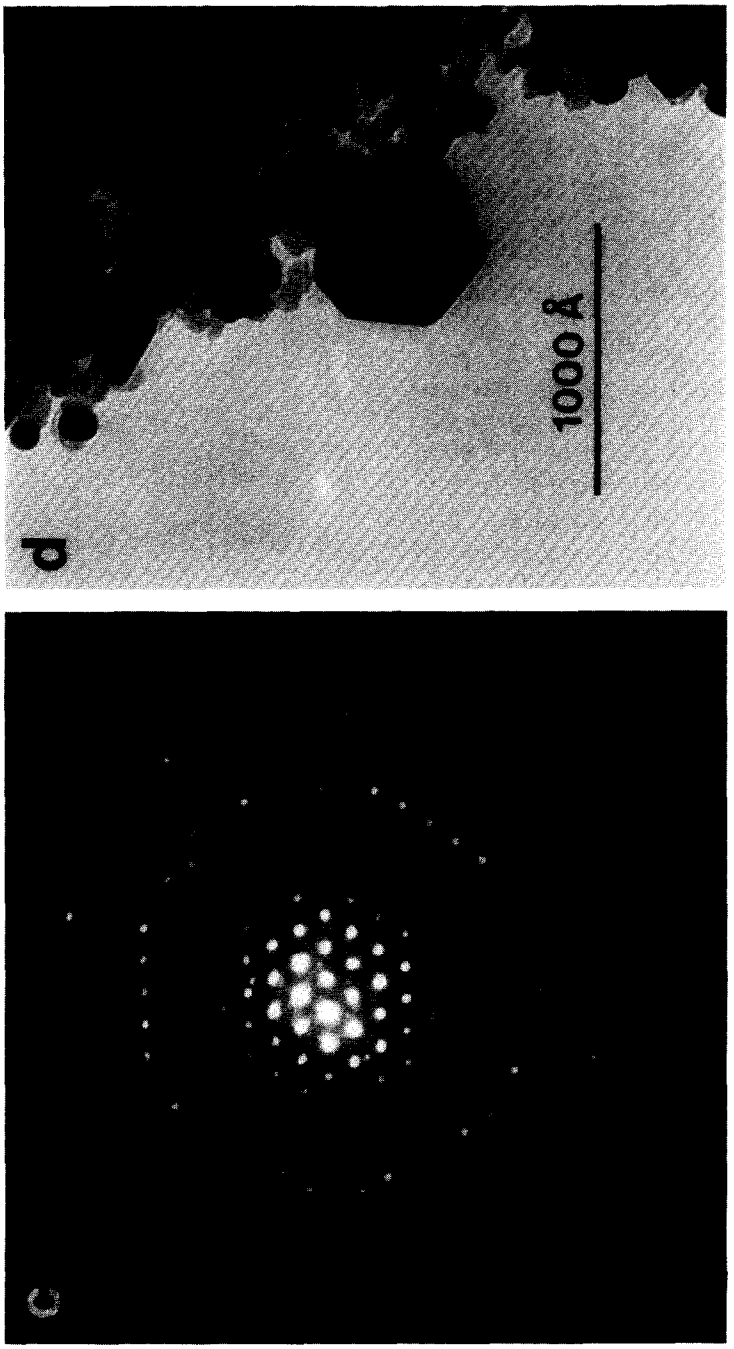

FIG. 8. Convergent beam diffraction (CBD) of abnormally large particles. (a) CBD pattern; (b) bright field micrograph of particle; (c) CBD pattern; (d) bright field micrograph of particle.

patterns. As a result, difficulty was encountered in obtaining patterns from particles smaller than ~200 Å.

Figures 8a and c show two convergent beam patterns obtained from the particles shown in Figs. 8b and d, respectively. Figure 8a corresponds to a Pt [110] pattern, while Fig. 8c indexes as [111] with extra spots of the type $\frac{1}{3}$ {422}, or alternatively might be interpreted as [112] with extra $\frac{1}{2}$ {311} spots. This pattern (Fig. 8c) is similar to those from large platinum particles reported in the recent study of an alumina-supported catalyst by Roth (*22*). There are several possible explanations for the origin of the extra spots. They include multiple diffraction from either side of a boundary or boundaries normal to the beam direction (*22, 41*), an atomically stepped surface (*42*), or an array of dislocations at a partially coherent interface. Calculations of the relative electron diffraction intensities to be expected from each of these models indicate that none of them is likely to be the complete explanation. In general, a better structural characterisation of the anomalously large particles might be expected to provide an understanding of the mechanisms by which they grow preferentially.

X-ray microanalysis was used to confirm that the large particles contained platinum. Figure 9a illustrates the relative intensities of the Pt and Al peaks in the X-ray spectrum from a wide area (~1000 μm^2) of catalyst. Figure 9b shows the greatly increased relative intensity of the Pt peak obtained when the probe was focused on the particle shown in Fig. 8d.

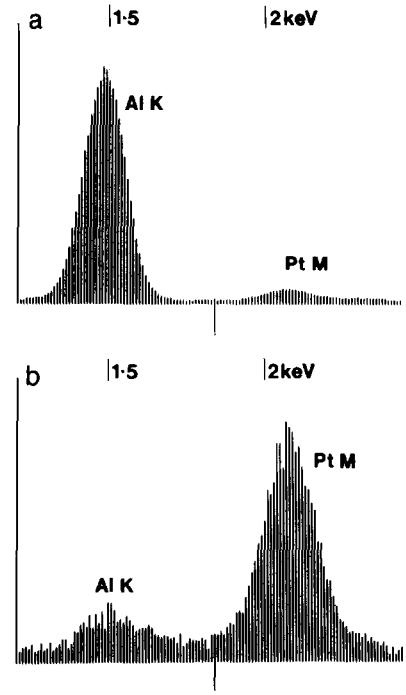

FIG. 9. Pt and Al peaks in energy-dispersive X-ray (EDX) spectrum of Pt/Al_2O_3 heated for 24 hr in air at 600°C. (a) General region; (b) probe focused on particle shown in Fig. 8d.

Surface Area Measurements

In Table 2 the values of d_s, the surface average diameter, determined by H_2 adsorption and TEM are compared. The error on TEM determination of d_s from a sample of 1000 particles was found to be approximately ±5% (the error for fresh specimens is smaller since a larger sample was measured), and the uncertainly on adsorption measurements was ±10%. It can be seen from the table that the difference between the two sets of d_s values is in each case within the range of the quoted errors. This would suggest that the platinum particle size distribution in TEM specimens was broadly representative of those in Fecralloy-supported catalysts.

CONCLUSIONS

A new technique for the preparation of supported metal catalyst TEM specimens,

TABLE 2

Values of Surface Average Diameter Determined by TEM and H_2 Adsorption

Sintering time (hr)	d_s (Å) TEM	d_s (Å) H_2 Adsorption
0	68.2 ± 2.4	60 ± 6
2	98.6 ± 4.9	90 ± 9
8	119 ± 6	122 ± 12
24	174 ± 9	164 ± 16

based on the sol-gel process, has been developed. For the particular catalyst studied here, a commercial platinum/alumina catalyst, the new technique has a number of advantages over traditional specimen preparation techniques. Large thin regions can readily be produced without any modification of catalyst structure: the necessity to grind or section the catalyst is also avoided. No carbon film is required, so individual specimens may be subjected to repeated heat treatments in oxidizing environments. This is not only convenient, but also enables examination of the same area before and after sintering, a possibility which is being explored in further studies (*43*). Information concerning the distribution of catalyst particles with respect to the support morphology is also available with the new technique. The technique is simple, and large numbers of high-quality specimens can be produced in a relatively short time. Surface area measurements carried out by H_2 adsorption have indicated that the regions examined by TEM were representative of the overall catalyst.

Catalyst specimens have been sintered in air at 600°C, a typical temperature of operation for a catalyst in an automobile exhaust system. A consideration of particle size distributions in sintered catalysts has led to the conclusion that a change in the predominant sintering mechanism from particle migration and coalescence to interparticle transport occurs after approximately 2 hr, when the mean particle size is 73.5 Å. For periods longer than about 8 hr sintering occurs chiefly through the growth of "abnormally large" particles which are often facetted and sometimes plate-like in character. A decrease in the sintering power-law exponent from ~14 to ~7 confirms that a change in mechanism occurs. Convergent beam diffraction patterns of fast-growing particles are consistent with platinum metal, showing that these particles do not result from, say, a reaction between metal and support. Extra spots in some of the diffraction patterns suggest that some of these large particles may have a twinned structure. Smaller particles containing twin boundaries have been observed in bright field images of fresh and sintered catalysts.

ACKNOWLEDGMENTS

The TEM specimen preparation technique described in this paper was originally brought to our attention by D. J. Mazey of the Metallurgy Division, AERE Harwell, to whom grateful thanks are expressed. Gratitude is also due to G. Butler and P. S. Drew of the Catalyst Unit, AERE Harwell, for expert assistance with surface area measurements. L. Stoter of Philips Analytical helped to record the electron diffraction pattern reproduced in Fig. 8a.

Financial support from the Science Research Council and AERE Harwell for a CASE studentship (P.J.F.H.) is gratefully acknowledged.

REFERENCES

1. Dalla Betta, R. A., McCune, R. C., and Sprys, J. W., *Ind. Eng. Chem. Prod. Res. Dev.* **15,** 169 (1976).
2. Ruckenstein, E., and Pulvermacher, B., *AIChE J.* **19,** 356 (1973).
3. Ruckenstein, E., and Pulvermacher, B., *J. Catal.* **29,** 224 (1973).
4. Granqvist, C. G., and Buhrman, R. A., *J. Appl. Phys.* **47,** 2200 (1976).
5. Wynblatt, P., and Gjostein, N. A., *Prog. Solid State Chem.* **9,** 21 (1975).
6. Wynblatt, P., and Gjostein, N. A., *Acta Met.* **24,** 1165 (1976).
7. Wynblatt, P., *Acta Met.* **24,** 1175 (1976).
8. Flynn, P. C., and Wanke, S. E., *J. Catal.* **34,** 390 (1974).
9. Flynn, P. C., and Wanke, S. E., *J. Catal.* **34,** 400 (1974).
10. Wynblatt, P., and Gjostein, N. A., *Scripta Met.* **7,** 969 (1973).
11. Chu, Y. F., and Ruckenstein, E., *J. Catal.* **55,** 281 (1978).
12. Baker, R. T. K., Thomas, C., and Thomas, R. B., *J. Catal.* **38,** 510 (1975).
13. Baker, R. T. K., Prestridge, E. B., and Garten, R. L., *J. Catal.* **56,** 390 (1979).
14. Baker, R. T. K., Prestridge, E. B., and Garten, R. L., *J. Catal.* **59,** 293 (1979).
15. Chen, M., and Schmidt, L. D., *J. Catal.* **55,** 348 (1978).
16. Ahn, T. M., Wynblatt, P., and Tien, J. K., *Acta Met.* **29,** 921 (1981).
17. Wilson, G. R., and Hall, W. K., *J. Catal.* **17,** 190 (1970).
18. Flynn, P. C., and Wanke, S. E., *J. Catal.* **37,** 432 (1975).

19. Furhman, Z. A., and Parravano, G., Proc. Int. Congr. Catal. 6th (London 1976), p. 686. Chemical Society, London, 1977.
20. Dautzenberg, F. M., and Wolters, H. B. M., *J. Catal.* **51,** 26 (1978).
21. Mustard, D. G., and Bartholomew, C. H., *J. Catal.* **67,** 186 (1981).
22. Roth, L. D., Doctor of Engineering Science Thesis, Columbia University, 1981.
23. Adams, C. R., Benesi, H. A., Curtis, R. M., and Meisenheimer, R. G., *J. Catal.* **1,** 336 (1962).
24. Freel, J., *J. Catal.* **25,** 139 (1972).
25. Moss, R. L., *Platinum Metals Rev.* **11,** 141 (1967).
26. Nelson, R. L., Ramsay, J. D. F., Woodhead, J. L., Cairns, J. A., and Crossley, J. A. A., *Thin Solid Films* **81,** 329 (1981).
27. Desport, J. A., Moseley, P. T., and Williams, D. E., *J. Mater. Sci. Lett.* **1,** 288 (1982).
28. Cooper, B. J., *Platinum Metals Rev.* **19,** 141 (1975).
29. Flynn, P. C., Wanke, S. E., and Turner, P. S., *J. Catal.* **33,** 233 (1974).
30. Treacy, M. M. J., and Howie, A., *J. Catal.* **63,** 265 (1980).
31. Steeds, J. W., *in* "Introduction to Analytical Electron Microscopy" (J. J. Hren, J. I. Goldstein, and D. C. Joy, Eds.), p. 387. Plenum, New York, 1979.
32. Drew, P. S., and Haines, M. J., AERE (Harwell) Report No. M3187 (1981).
33. Pratt, A. S., and Cairns, J. A., *Platinum Metals Rev.* **21,** 74 (1977).
34. Cairns, J. A., Nelson, R. S., and Acres, G. K., *Mater. Eng. Appl.* **1,** 162 (1979).
35. Avery, N. R., and Sanders, J. V., *J. Catal.* **18,** 129 (1970).
36. Marks, L. D., and Howie, A., *Nature (London)* **282,** 196 (1979).
37. Gruber, E. E., *J. Appl. Phys.* **38,** 243 (1967).
38. Kuo, H. K., Ganesan, P., and de Angelis, R. J., *J. Catal.* **64,** 303 (1980).
39. Pennycook, S. J., *J. Microsc.* **124,** 15 (1981).
40. Lynch, J. P., Lesage, E., Dexpert, H., and Freund, E., EMAG 81, Inst. Phys. Conf. Ser. No. 61, 67 (1981).
41. Morriss, R. H., Bottoms, W. R., and Peacock, R. G., *J. Appl. Phys.* **39,** 3016 (1968).
42. Cherns, D., *Phil. Mag.* **30,** 549 (1974).
43. Harris, P. J. F., to be published.